Numerical investigation of disc-wing MAV with propeller in a wing slot

N. D. Ageev,
Department of Aeromechanics and Flight Engineering of
Moscow Institute of Physics and Technology, Gagarin 16, Zhukovsky

ABSTRACT

Concept of disc-wing MAV with propeller in a wing slot has a number of advantages and disadvantages. The concept is used by MIPTEAM for solving the problem of fixed wing MAV indoor flight by means of lift maximization for wing with low aspect ratio. There are only few investigations of disc-wing MAV aerodynamics with propeller in a wing slot. Present work describes numerical investigation technique and aerodynamic characteristics obtained. The main results are: good stall characteristics of this concept, low lift/drag ratio (further improvement is possible) and sophisticated flow pattern. It was obtained that the main part of the lift is created by wing surface in front of the actuator disk. Also, leading edge separation area produces small impact at the lift even at high angles of attack. It was found that increasing of the propeller thrust decreases maximum lift/drag ratio. Flow features in numerical results correspond to the known experimental results and flight tests.

1 INTRODUCTION

1.1 Background

A disk wing provides maximum surface and, consequently, takeoff weight (at equal other conditions) at the fixed lateral dimension. So, it is of the great interest for the usage in MAV. The experimental aircraft with fixed disk wing was presented by MIPTEAM at the Indoor Dynamics Competition during the IMAV-2010 [1] (Figure 1). Its maneuverability is provided by three factors: usage of the low aspect ratio wing, low wing load and propeller-wing interaction that needs further investigation [2].

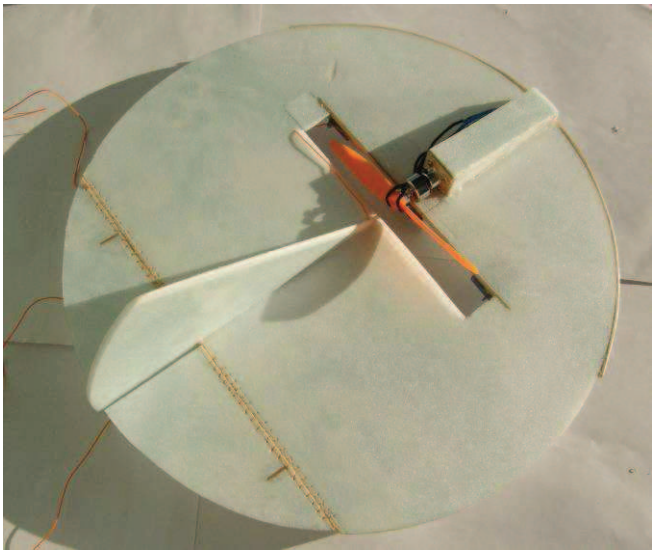

Figure 1: Disk-wing aircraft presented by MIPTEAM

Email address: n.d.ageev@gmail.com

Engineering methods along with flight experiment are usually used for calculation and improvement of the aircraft performance.

Further aerodynamic improvement of the apparatus requires more information about the flow pattern around the aircraft. Flow pattern can be obtained from experimental data (for example, by means of PIV) or from numerical modeling [3], [4]. Practically there are no experimental or numerical investigations of the disk-wing aircraft with the air screw situated at the slot in the wing. Therefore, numerical investigation technique is of great practical importance.

1.2 Notations

The following system of aerodynamics coefficients and approximations is accepted in this article:

L – Lift force
D – Drag force
F – Propeller thrust
M – Mass of the aircraft
V – Flight speed
P – Static pressure
ρ – Air density
q – Initial dynamic pressure ($q = 0.5\rho V^2 = 14.8125$ Pa)
α – Angle of attack (AoA)
S – Characteristic area ($S = 0.25\pi diameter^2 = 0.012$ m^2)
C_L – Lift Coefficient; $L=C_L qS$
C_D – Drag Coefficient; $D=C_D qS$
C_{D0} – Drag coefficient at zero lift
C_P – Pressure coefficient; $C_P = (P-P_\infty)/q$
C_L (C_D) is approximated by $C_D = C_{D0}+A_1 C_L+A_2 C_L^2$

2 PROBLEM FORMULATION

2.1 General formulation

The problem is to calculate aerodynamics coefficients and flow pattern around the aircraft, represented by MIPTEAM [1], at the velocity equal to an average flight speed of the apparatus at the IMAV-2010. The characteristic time of every IMAV lap is 8 seconds. Length of the lap is about 40 m, average flight speed V = 5 m/s. Reynolds number calculated at the chord of the wing (equal to 0.3 m) is 103 300. An estimate of the air screw thrust is also required. For the apparatus with mass M = 70 g with a C_L/C_D ratio 3.5 the required thrust is 0.2 N. The flight throttle is known to be about 40% of maximum thrust (F_{max} = 0.5 N). These two estimates agree well and give a thrust F = 0.2 N. After preliminary calculations it was found that the required thrust in cruise mode was higher than estimated, second stage of calculations was carried out with thrust F = 0.324 N.

2.2 *Geometric model and mesh*

The geometry of the apparatus was simplified (final geometry is shown in Figure 2). Control surfaces are fixed. The propeller is simulated by an actuator disk according to [4]. Thus, swirling of the propeller stream wasn't considered in the work.

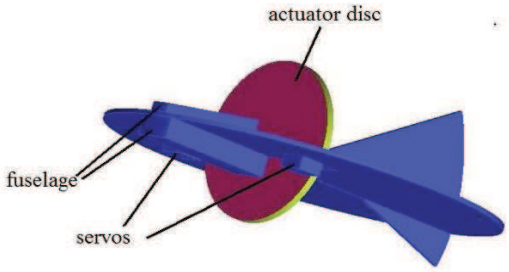

Figure 2: Geometric model

The thickness of the actuator disk is equal to the maximum thickness of the propeller. Computational domain around the unit has dimensions 20x20x20 diameters of the wing. The model unit is located in the center of the computational domain. The selected size of the computational domain provides correct simulation of the vortex system of the wing at an acceptable computing cost.

Computational domain contains unstructured tetrahedral mesh with prismatic layers (Figure 3). This type of the mesh provides satisfactory quality of the flow separation simulation. The size of the cells on the model surface doesn't exceed 2 mm. General maximum cell size is equal to 128 mm. The cell size growth ratio is 1.08, which provides sufficiently detailed simulation. The total grid has 6 677 448 elements. Volume mesh is generated from surface mesh by improved Delaunay algorithm. There are 91 220 elements on the surface of the aircraft (without disk) and 14 473 elements at the surfaces of the actuator (which is much more then used in [4]). Prism layers are created on the surface of the model. Total thickness of the prism layer is 2.58 mm, which provides careful simulation of the boundary layer at given Reynolds number (103 300). Prism layer provides $Y+max$=3.56.

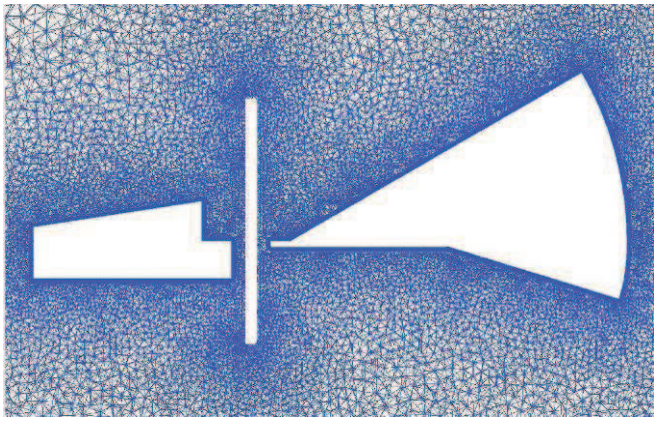

Figure 3: Mesh around the model

Test calculations showed good agreement between the results from this mesh and mesh with 14 millions elements.

2.3 *Boundary conditions*

Boundary conditions on the walls of the computational domain are standard: front and bottom walls of the computational domain - inlet, rear and top – outlet, side – free slip wall. The air screw is modeled by an outlet at the front surface of the actuator, inlet at the rear surface. Mass flow rate is set through the actuator corresponding to the speed at the propeller, calculated by the theory of the active disk [5]. The side wall of the actuator is a free slip one. As shown by test calculations, this method allows the simulation of the propeller to be accurate enough to simulate thrust with preserving the continuity of the velocity through the actuator. Stream swirling is neglected in this approximation.

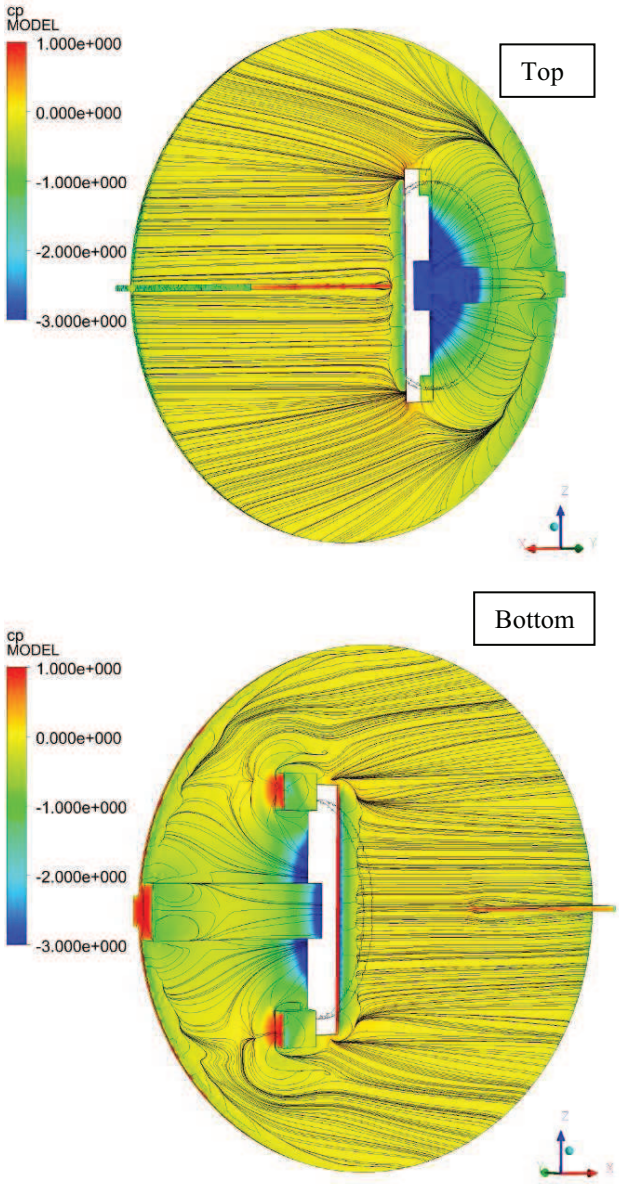

Figure 4: C_p distribution and surface shear stress streamlines at zero angle of attack

3 SOLUTION, VERIFICATION AND VALIDATION

3.1 *Solution*

RANS system of governing equations with the SST turbulence model was solved by the solver ANSYS CFX™.

Solving is carried out with an incompressible viscous fluid model with parameters corresponding to air at 25C.

The problem is solved in a stationary regime with the approximation scheme of the second-order. One calculation takes 750 iterations in average. Stop condition is fixation of the third significant digit in magnitude of the aerodynamic forces acting at the model.

Preparation for calculations took near two weeks, one point extraction took 7 hours of calculation time at i7-960 (3.0 GHz, 4 physical cores) processor.

3.2 Verification

For verification shear stress lines are built on the model surface at zero angle of attack (Figure 4).

General flow pattern (at all investigated AoA) is in good accordance with experimental data [6]. Flow separation regions near sharp edges are simulated. Performance of the actuator stream corresponds to the active disk theory [5] qualitatively: the jet narrows both in front and besides of the actuator. Vortex system of the wing is present at any non-zero angle of attack and can be visualized by pressure isosurface with low static pressure (Figure 5). Distance of the vortex system trace modeling is large enough (about 2 m).

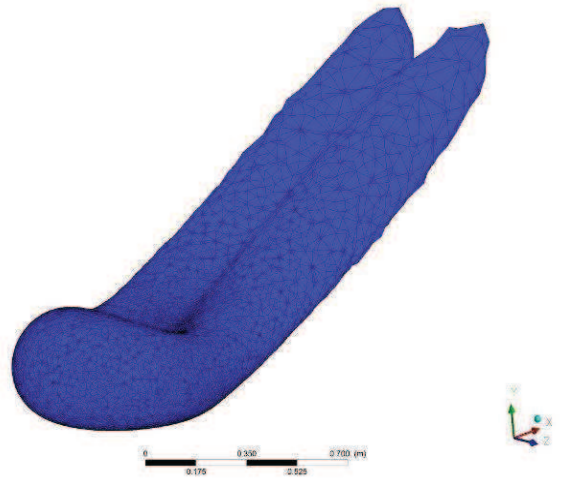

Figure 5: Isosurface of low pressure around the model at 40 degrees angle of attack

Boundary layer is simulated at all the surface of the wing. Low velocity areas besides the model are observed. Thus, the data agree well with the theory predictions and experiment [6], and can be subjected to further analysis.

3.3 Validation

Results of the computations show the good accordance between average pressure drop (that is about 25 Pa) on the actuator and the propeller thrust F=0.324N. Magnitude of the calculated lift of the vehicle let it fly stable at the angle of attack of 15 degrees and even perform aerobatics, as it was seen at the IMAV-2010. A_2=*0.4225* calculated for the angles of attack 0-20 degrees is also in a good accordance with the experimental data obtained in [7] (A_2=*0.45* for this wing).

4 RESULTS

C_L *(*C_D*)* function is shown in Figure 6. C_{D0}=0.2 is greater than estimated for this type of MAV (C_{D0}=0.03...0.1). The main part of the C_{D0} is pressure drag (about 85%). Large pressure drag can be explained by influence of the fuselage, servos, blunt edges with sharp corners and slot around the propeller.

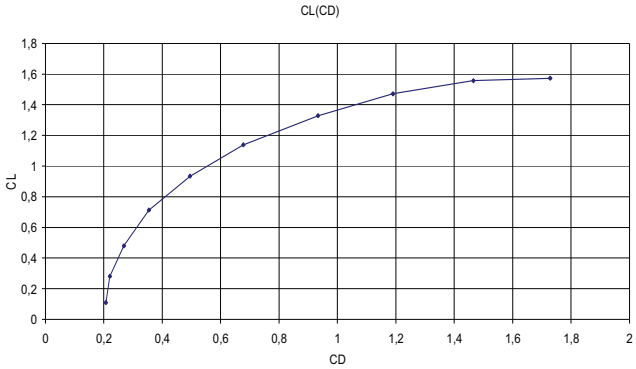

Figure 6: C_L as function of C_D

As one can see, the greatest values of the pressure are at leading edges of the wing and fuselage and at the leading slot edge.

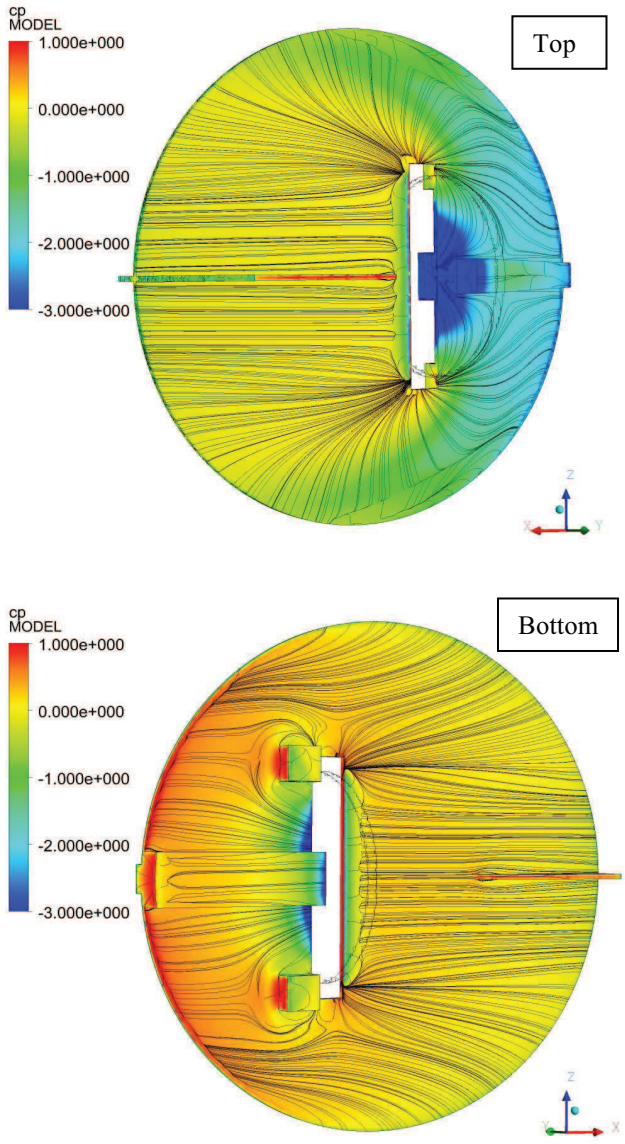

Figure 7: C_p distribution and surface shear stress streamlines at angle of attack of 15 degrees

Pressure distribution along with shear stress streamlines at cruise angle of attack (15 degrees) is shown in Figure 7. The static pressure decrease at the rear fuselage and servo surfaces is also caused by propeller work.

Thus, great amount of the drag at the wing is induced by propeller.

The air screw also loses some thrust due to low-speed zones besides the fuselage and the wing.

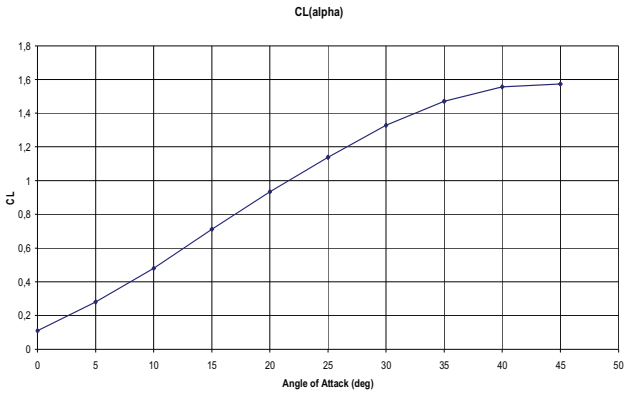

Figure 8: C_L as function of Angle of Attack

One of the most important results obtained is that the C_L (C_D) function coefficient A_2 calculated for the angles of attack 0-20 degrees is 0.4225 that is in a good agreement with the experimental data (0.45) [7]. But at the high angles of attack the A_2 becomes greater. It is caused by the intensification of the vortices and increase of the vortex lift role that can be proved by comparison of the flow patterns at different angles of attack and by investigation of the C_L as function from angle of attack. As it was expected, C_L (α) dependence has increasing derivative at angles of attack near 5-15 degrees (Figure 8). Non-zero lift at zero AoA is associated with an asymmetric air screw position relative to the longitudinal axis of the aircraft (air screw center is higher than the longitudinal axis; C_p distribution at zero AoA is shown in Figure 4).

Stall comes at the angle of attack near 45 degrees that is good, but perhaps can be better. Separation zones at this AoA are the largest ones. Thus, flow pattern at this angle of attack is the most interesting.

Flow structure above the wing at the angle of attack 40 degrees is visualized by the pressure distribution and shear stress surface streamlines in Figure 9. The flow has three main features: a strong vortex system of the wing (can be observed in Figure 5), low lift at the wing surface besides the airscrew and weak effect of the leading edge separation (at C_P distribution and consequently C_L).

Strong vortex system of the wing is concerned with the low aspect ratio and the propeller-wing interaction. It increases AoA of stall, but decreases the C_L/C_D ratio.

Small lift at the wing area situated besides the air screw is associated with the rectifying of the flow besides the propeller and has three consequences. At first, total lift decreases. The other consequence is that aerodynamic focus shifts closer to the leading edge that makes the aircraft less stable. And the last consequence is that center of aerodynamic force application shifts to the leading edge, that reduces balance loses. So, this problem requires further investigation.

Little effect of the leading edge primary separation is concerned with the influence of the vortex system that creates a reverse flow zone in front of the wing and provokes a secondary separation besides of the primary one. Thus, efficiency of the deflected leading edge requires further investigation.

C_L/C_D ratio as function of C_L is presented in Figure 10. One can see that flight at the IMAV-2010 was carried out at the regime close to the maximum C_L/C_D mode. Low magnitude of the maximum C_L/C_D ratio caused by two reasons: high C_{D0} and high A_2 of the vehicle. The first reason is concerned with the drag of the blunt fuselage around the airscrew that can be reduced by slight geometry modification, the second one – with low aspect ratio that can't be sufficiently changed by geometry modification (in the concept of maximum lift at the fixed lateral dimension).

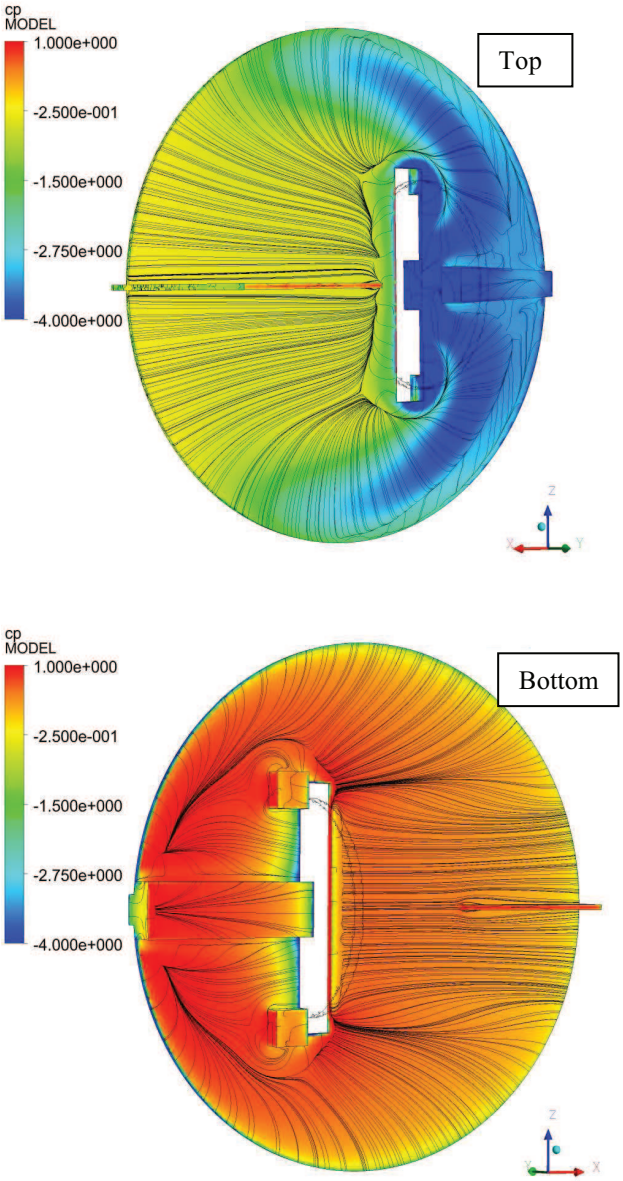

Figure 9: C_p distribution and surface shear stress streamlines at angle of attack of 40 degrees

If F=0.2N maximum C_L/C_D ratio is equal to 2.4 and is reached at lower AoA, C_{D0}=0.12 that confirms existing of the relationships between the C_{D0}, A_2 and the propeller thrust.

5 CONCLUSION

Good agreement between the results obtained and experimental/flight test data is reached. Some interesting flow features around the vehicle are extracted: vortices, flow separation areas and small lift area besides of the actuator disk. The last feature requires further complex (dynamic and aerodynamic) investigation.

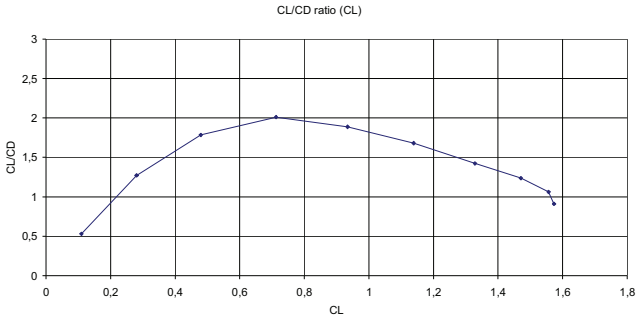

Figure 10: C_L/C_D ratio as function of C_L

Leading edge separation produces small impact at the lift of the vehicle. Increasing the propeller thrust reduces maximum C_L/C_D ratio. It is obtained that the lift can provide maneurability of the apparatus. Main aerodynamic relationships were obtained and can be used in further aerodynamic research and development. It was found that further work on reducing the C_{D0} is appropriate. Howewer, in the model used for calculations propeller stream was simplified by means of jet without swirling.

ACKNOWLEDGMENT

The present work is carried out under support of Russian "UMNIK" program. The author is grateful to prof. S. V. Serokhvostov, prof. I. V. Voronich, prof. A. A. Pavlenko and E. V. Birukova for the preliminary remarks.

REFERENCES

[1] MAV Book. *IMAV-2010 proceedings.* Braunschweig, 2010

[2] N. D. Ageev. Design of a highly maneuverable MAV able for controlled indoor flight. *Proceedings of the 53rd conference MIPT "Modern problems of fundamental and applied sciences" Part 6. Aeromechanics and Flight Engineering.* - Moscow: MIPT, 2010. p. 97-98. (in Russian)

[3] Mark Groen, Bart Bruggeman, Bart Remes, Rick Ruijsink, Bas van Oudheusden, Hester Bijl. Improving Flight Performance of the Flapping Wing MAV DelFly II. *IMAV-2010 proceedings.* Braunschweig, 2010

[4] Sungjin Choi and Jon Ahn. A Computational Study on the Aerodynamic Influence of a Pusher Propeller on a MAV. AIAA 2010-4741. *40th Fluid Dynamics Conference and Exhibit 28 June - 1 July 2010, Chicago, Illinois*

[5] Glauert, H. The elements of aerofoil and airscrew theory-2nd ed. – (Cambridge Science Classics Series), 1983, Cambridge University Press

[6] J. R. Potts, W. J. Crowther. Visualization of the flow over a disc wing. *9th International Symposium on Flow Visualization, Heriot-Watt University, Edinburgh, 2000*

[7] A. V. Kornushenko, S. V. Serokhvostov. Experimental studies of the aerodynamics of miniature aircraft. *"Air Fleet Tech"* № 2-2008 p. 6-9. Moscow: TsAGI, 2008 (in Russian)